

Molecular Dynamics Study of Wetting of a Pillar Surface

Mathias Lundgren,* Neil L. Allan, and Terence Cosgrove

School of Chemistry, University of Bristol, Cantock's Close, Bristol BS8 1TS, United Kingdom

Neil George

Syngenta, P.O. Box A38, Leeds Road, Huddersfield,
West Yorkshire HD2 1FF, United Kingdom

Received February 10, 2003. In Final Form: May 16, 2003

We present results of molecular dynamics simulations of water droplets at pillar surfaces comprised of sheets of carbon atoms. We examine variations in the contact angle with the height of the pillars. A crossover is observed between the Wenzel and Cassie–Baxter regimes when the height of the pillar is changed.

Introduction

Wetting of a water droplet on a perfectly smooth ideal surface is described by Young's equation. However, all real surfaces are rough to some extent, and this changes the wettability considerably. It is crucial whether water molecules interact with all the solid substrate by penetrating the hollows. If the liquid does penetrate and the surface is dry ahead of the contact line, a useful approximation is that of Wenzel¹ who modified Young's equation such that the contact angle, θ , is altered by a roughness factor, r :

$$\cos \theta = r \cos \theta_0 \quad (1)$$

where θ_0 is the contact angle for a perfectly smooth surface.

If air is trapped in the hollows on the rough surface the liquid is only in contact with the "upper" part of the surface and the droplet remains almost spherical ($\theta \rightarrow 180^\circ$). Wenzel's approximation then fails and an alternative treatment starting from Young's equation is that of Cassie and Baxter.² They considered the contact angle at heterogeneous surfaces composed of two different materials, for which the separate contact angles are θ_1 and θ_2 . If the second of these is air, the contact angle θ_2 is 180° , and

$$\begin{aligned} \cos \theta &= f \cos \theta_1 + (1 - f) \cos \theta_2 \\ &= f \cos \theta_0 + (1 - f) \cos 180^\circ \\ &= f(\cos \theta_0 + 1) - 1 \end{aligned} \quad (2)$$

where f and $1 - f$ are the fractional areas of the wetted solid/liquid and liquid/air interfaces, respectively.

An example of the effect of surface roughness is the highly repellent fluorinated surface with a well-controlled pillar structure, studied by Yoshimitsu et al.³ The experimental contact angles for water on this surface are $>150^\circ$ and vary with the pillar height and width. For low roughness, Wenzel's regime is followed with a marked

increase in the contact angle with roughness. At high roughness, when the height of the pillars is increased, the gaps between them are filled with trapped air rather than liquid. The increase in height, thus, has only a small effect on the contact angle, which remains effectively constant in agreement with Cassie and Baxter. These super hydrophobic surfaces, with contact angles close to 180° , have been widely discussed,^{3–6} and it appears that such surfaces must have the appropriate surface roughness and geometry. In this paper, we present results of molecular dynamics simulations of wetting of an anisotropic pillarlike surface consisting of sheets of hexagonally arranged carbon atoms. The results are compared with recent simulations on wetting at an atomistic flat surface.⁷

Methods

The model is a *full* atomistic representation and includes long-range electrostatic interactions. The potentials and charges used to describe the water molecules were taken, as in our previous work on the behavior of water/ethanol droplets on a graphite surface,⁷ from the TIP-3P model of Jorgensen et al.⁸ The short-range intermolecular interactions are all of the Lennard–Jones form with a cutoff at 9 Å. Values of the Lennard–Jones parameters σ and ϵ for the surface carbon atoms are taken from the Optimized Potentials for Liquid Simulations force field,⁹ and the Lorentz–Berthelot geometric mixing rules were used to determine the surface/water potential parameters. The long-range Coulombic interactions were handled by direct summation with a cutoff distance larger than the drop radius. The program DL_POLY¹⁰ was used for the molecular dynamics simulations, which were performed at a constant volume and temperature (NVT). The temperature was set to 298 K and kept constant using the Berendsen thermostat.¹¹ The simulations were carried out with a time step of 1 fs. The typical lengths of the production runs were 500 ps.

(4) Extrand, C. W. *Langmuir* **2002**, *18*, 7991.

(5) Chen, W.; Fadeev, A. Y.; Hsieh, M. C.; Oner, D.; Youngblood, J.; McCarthy, T. J. *Langmuir* **1999**, *15*, 3395.

(6) Oner, D.; McCarthy, T. J. *Langmuir* **2000**, *16*, 7777.

(7) Lundgren, M.; Allan, N. L.; Cosgrove, T. *Langmuir* **2002**, *18*, 10462.

(8) Jorgensen, W. L.; Chandrasekhar, J.; Madura, J. D.; Impey, R. W.; Klein, M. L. *J. Chem. Phys.* **1983**, *79*, 926.

(9) Jorgensen, W. L.; Maxwell, D. S.; Tirado-Rives, J. *J. Am. Chem. Soc.* **1996**, *118*, 11225.

(10) Forester, T. R.; Smith, W. *DL_POLY*; CCLRC Daresbury Laboratory: Warrington, England, 1995.

(11) Berendsen, H. J. C.; Postma, J. P. M.; Vangunsteren, W. F.; Dinola, A.; Haak, J. R. *J. Chem. Phys.* **1984**, *81*, 3684.

* Author to whom correspondence should be addressed. E-mail: mathias.lundgren@bristol.ac.uk.

(1) Wenzel, R. N. *Ind. Eng. Chem.* **1936**, *28*, 988.

(2) Cassie, A. B. D.; Baxter, S. *Trans. Faraday Soc.* **1944**, *40*, 546.

(3) Yoshimitsu, Z.; Nakajima, A.; Watanabe, T.; Hashimoto, K. *Langmuir* **2002**, *18*, 5818.

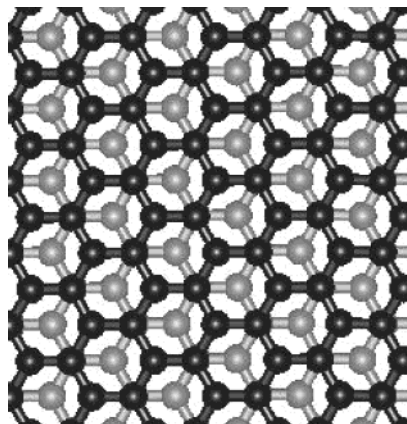


Figure 1. Top view of one pillar, showing how the carbon sheets are layered. The black color represents a top atom layer while the gray atoms are located in the lower layers.

The smooth, flat, solid slab consisted of three layers of carbon atoms hexagonally arranged as in graphite, separated by 1.42 Å and with a surface number density of 0.384 Å⁻². The sheets of atoms were separated by 3.4 Å and stacked as shown in Figure 1. The pillar surface was constructed from a similar slab consisting of layers of carbon atoms, from which pillars were constructed by removing the appropriate atoms. Each pillar is a cuboid with a side of 12 Å. The height of the pillar was varied from 3.4 to 61.4 Å. All surface atoms were kept fixed in position during the simulations.

The liquid phase was set up by "cutting out" a spherical droplet with a radius of 20 Å (33.5 nm³), approximately 1100 water molecules, from a simulation cell of equilibrated bulk water. The equilibrated water droplet was placed on top of the solid surface, and when the simulation started, the droplet began to wet the surface spontaneously. Wetting properties were calculated as described previously.⁷

Results and Discussion

In previous simulations⁷ of a water droplet on top of a perfectly smooth {0001} graphite surface, the water droplet wetted the surface with a contact angle of 83.3 ± 5.3°, which is close to the macroscopic experimental value.¹² For comparison, we have carried out similar simulations on the perfectly smooth surface formed by cleaving vertically through the layers of the slab. This surface is identical to the walls of the pillars. Because the atom density is lower for this surface, the droplet spreads out less and the contact angle calculated to be 111 ± 3.2° is larger than that for the {0001} surface.

The wetting properties change considerably for the pillar structure. Figure 2 shows the time dependence of the distance of the center of mass of the droplet perpendicular above the surface with pillars of a height of 10.2 Å. The spreading mechanism for this surface can be divided into three stages. During the initial stage of the simulation, the drop moves down from its original position until it makes contact with the surface (Figures 3a and 4a). In the second stage, it spreads out and slides over the top of the pillars without penetrating the gaps between them. The wettability of the top of the pillars is higher than that at the walls, so first the drop maximizes the contact with the top of the pillars. The preferred configuration of the droplet is such that it covers four of the pillars. After the droplet attains its position on top of the pillars, in the third stage, water molecules begin to diffuse into the gaps between the pillars (Figures 3c and 4b). Eventually all of the hollow is occupied by the liquid. The estimated contact

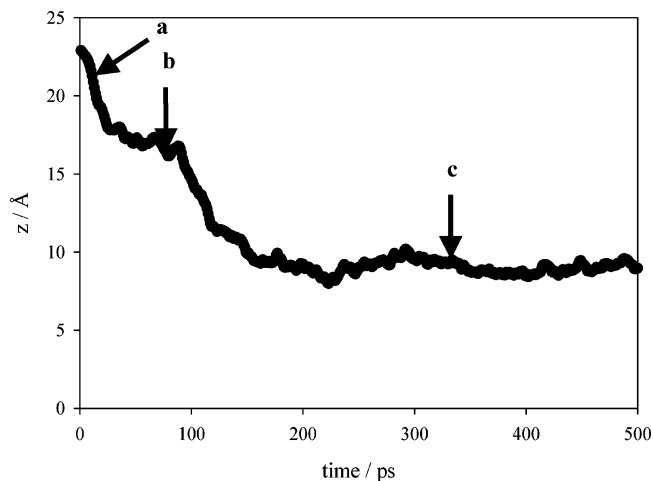


Figure 2. Evolution of the center of mass of the droplet with time. The top of the pillars are located at $z = 0$. Parts a, b, and c refer to the three different stages of the wetting discussed in the text. The pillar height is 10.2 Å.

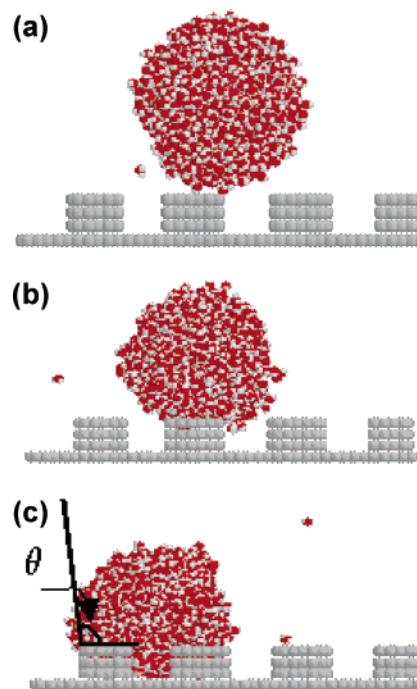


Figure 3. Snapshots from the simulations. Part a shows the initial configuration and position of the droplet. Part b shows the intermediate stage of the wetting procedure, where the droplet is wetting the top part of the pillars only. Part c is the final stable position of the droplet, where the water molecules have penetrated the pillars. The pillar height is 10.2 Å. The contact angle is determined, as shown, where the water is in contact with the top of the pillars, as described in ref 7.

angle after the spreading and penetration into the pillar surface is 110.8 ± 3.1°. This should be compared with the significantly lower value, 83°, for the smooth {0001} surface.

It is also of interest to investigate the effects of changing the pillar height. The equilibrium contact angle varies with the pillar height. Contact angles for a range of pillar heights, from 3.4 to 61.2 Å, have been calculated and are shown in Figure 5. There is a clear change of behavior between 10 and 20 Å, where the contact angles become essentially independent of the pillar height. As the height of the pillars increases beyond 20 Å, the water molecules do not penetrate the gaps between the pillars. The resulting final configuration of the droplet on top of

(12) Fowkes, F. M.; Harkins, W. D. *J. Am. Chem. Soc.* **1940**, *62*, 3377.

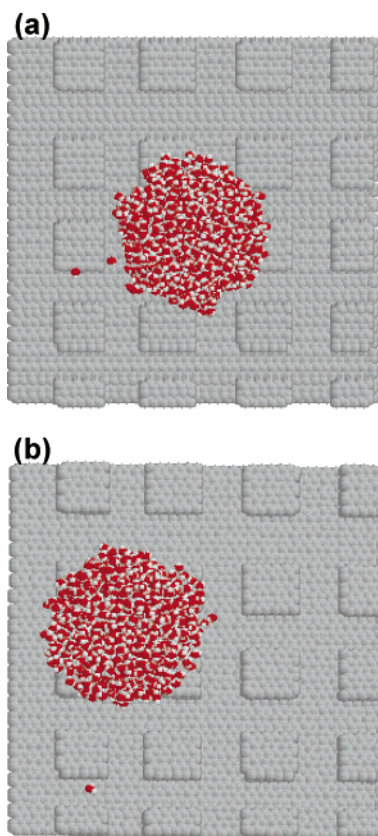


Figure 4. Part a illustrates a snapshot viewing the surface from above, showing the initial configuration of the droplet. Part b is a snapshot of the equilibrated water droplet on top of the pillar surface in equilibrium after spreading. The pillar height is 10.2 Å.

61.2 Å high pillars is, for example, shown in Figure 6. The droplet does not penetrate to the bottom of the gaps, and the calculated contact angle is $128.4 \pm 1.6^\circ$. This is considerably larger than the values for the separate surfaces, which make up the top and the sides of the pillar. We appear now to be in the Cassie and Baxter regime.

To sum up, our simulations have shown the effects of surface structure and density on wetting phenomena. The different wetting properties of the top and the sides of the pillars play an important role in determining the contact angle. The droplet spontaneously migrates from its randomly chosen nonequilibrium configuration to its final position, in which a stable droplet is formed on top of four pillars. For low pillar heights, the system is in the Wenzel regime and a change to that of Cassie and Baxter is seen when the pillar height was increased. The contact angles seem to be independent of the pillar height when h exceeds 15 Å. The contact angles depend on the topography of the surface. Both the pillar width and the gaps between the pillars are clearly important factors,⁶ and these will be

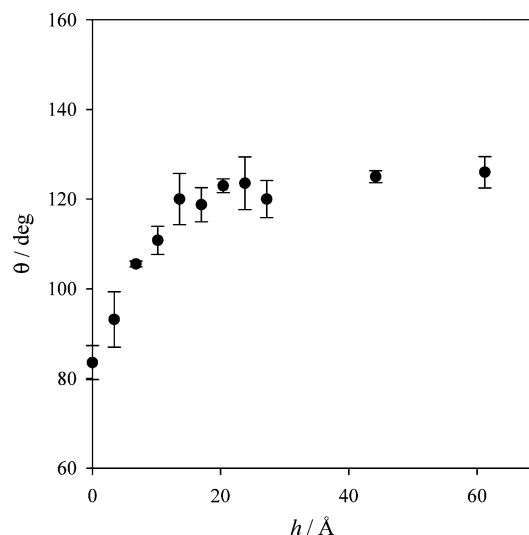


Figure 5. Variation of the contact angle with the pillar height for the carbon pillar surface.

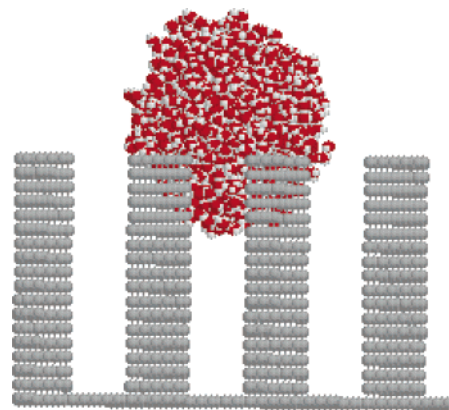


Figure 6. Snapshots from the simulation for a surface with tall pillars. The height of the pillars is 61.2 Å.

addressed in future publications. It is also likely that the sharp corners of the surface, where there is a particularly high density of atoms, also influence the wetting properties.

Molecular dynamics simulations are, thus, clearly able to provide a detailed insight at the atomic level into wetting phenomena. With calculations of this type, we can begin to tackle many related questions such as the role of defects, the effect of surfactants, and the dynamic processes associated with the formation of the final droplets.

Acknowledgment. We are grateful to EPSRC and Syngenta for financial support. Computational facilities were provided by two HEFCE JREI awards.

LA034224H